Antiviral Research xxx (2014) xxx–xxx

Contents lists available at ScienceDirect

Antiviral Research

journal homepage: www.elsevier.com/locate/antiviral

A screen of the NIH Clinical Collection small molecule library identifies potential anti-coronavirus drugs

Jianzhong Cao, J. Craig Forrest, Xuming Zhang *

Department of Microbiology and Immunology, University of Arkansas for Medical Sciences, Little Rock, AR 72205, United States

ARTICLE INFO

Article history:
Received 1 July 2014
Revised 8 October 2014
Accepted 20 November 2014
Available online xxxx

Keywords:
Coronavirus
Small molecule
NCC library
Screening

ABSTRACT

With the recent emergence of Middle East Respiratory Syndrome coronavirus in humans and the outbreak of devastating porcine epidemic diarrhea coronavirus in swine, therapeutic intervention is urgently needed. However, anti-coronavirus drugs currently are not available. In an effort to assist rapid development of anti-coronavirus drugs, here we screened the NIH Clinical Collection in cell culture using a luciferase reporter-expressing recombinant murine coronavirus. Of the 727 compounds screened, 84 were found to have a significant anti-coronavirus effect. Further experiments revealed that 51 compounds blocked virus entry while 19 others inhibited viral replication. Additional validation studies with the top 3 inhibitors (hexachlorophene, nitazoxanide and homoharringtonine) demonstrated robust anti-coronavirus activities (a reduction of 6 to 8 $\log_{10}$ in virus titer) with an IC_{50} ranging from 11 nM to 1.2 μM. Furthermore, homoharringtonine and hexachlorophene exhibited broad antiviral activity against diverse species of human and animal coronaviruses. Since the NIH Clinical Collection consists of compounds that have already been through clinical trials, these small molecule inhibitors have a great potential for rapid development as anti-coronavirus drugs.

1. Introduction

Coronavirus is an enveloped RNA virus. It has a single-strand, positive-sense RNA genome that is associated with nucleocapsid (N) protein to form the nucleocapsid inside the envelope (Fan et al., 2005; Jayaram et al., 2006). The spike protein protrudes from the virion surface to confer viral infectivity and is the major determinant of species- and tissue-tropism. Coronaviruses can infect humans and diverse species of animals, causing respiratory, digestive, neurological and immune-mediated diseases. Most human coronaviruses cause mild respiratory illnesses such as common cold or enteric diseases such as diarrhea (Caul and Egglestone, 1977; Resta et al., 1985; Zhang et al., 1994). But in 2003, a new coronavirus termed Severe Acute Respiratory Syndrome (SARS)-coronavirus suddenly emerged in the human population from wild animals (Drosten et al., 2003; Ksiazek et al., 2003; Marra et al., 2003; Rota et al., 2003), sickened more than 8000 people, and caused 774 deaths (CDC, 2004; Sorensen et al., 2006). Due to the fear caused by its ease of human-to-human transmission, disease severity and high mortality, the SARS outbreak posed a significant threat to public health and caused devastating economic loss. Fortunately, the epidemic subsided, and SARS has not re-emerged. However, another new coronavirus, termed Middle East Respiratory Syndrome (MERS) coronavirus, recently emerged in the Middle East and has now spread to dozens of countries (Lim et al., 2013; Mitka, 2013); it has infected more than 635 people and claimed 193 lives thus far (WHO, 2014). While the origins of SARS and MERS appear distinct, the respiratory disease similarities and high mortality rate has raised renewed concern about MERS' potential threat to public health on a global scale. Furthermore, although most of the existing animal coronaviruses are widespread, a new coronavirus strain, porcine epidemic diarrhea (PED) coronavirus, emerged several years ago in Asia and now has spread to the Americas, including the United States (Stevenson et al., 2013; Wang et al., 2014), causing significantly high mortality in affected piglets. This new epizootic disease has devastated the swine industry in these countries, having wiped out more than 10% of the U.S. pig population (De La Hamaide, 2014). However, to date, there is no effective drug available for treatment of any coronavirus infection, although a few drugs have been tested in vitro (Al-Tawfiq et al., 2014; Barlough and Shacklett, 1994; Falzarano et al., 2013; Morgenstern et al., 2005; Saijo et al., 2005).

* Corresponding author at: Department of Microbiology and Immunology, University of Arkansas for Medical Sciences, 4301 W. Markham Street, Slot 511, Little Rock, AR 72205, United States. Tel.: +1 (501) 686 7415; fax: +1 (501) 686 5359.
E-mail address: zhangxuming@uams.edu (X. Zhang).

http://dx.doi.org/10.1016/j.antiviral.2014.11.010
0166-3542/© 2014 Published by Elsevier B.V.

Table 1
Top anti-coronavirus drug candidates identified in DBT and 17Cl-1 cells.

Plate	Well	Sample_ID	Synonyms	Mean	SD	SSMD
Top candidates in DBT cells						
NCP002954	B10	SAM002554903	Hexachlorophene	1.1	0.2	−10.3
NCP002408	C11	SAM001246822	Homoharringtonine	1.2	0.1	−10.3
NCP002408	D06	SAM001246523	Duloxetine hydrochloride	4.6	0.2	−9.9
NCP003132	B04	SAM002699896	Mitoxantrone	4.7	0.5	−9.9
NCP002954	C09	SAM002554895	Chloroxine	5.9	0.5	−9.8
NCP003132	C05	SAM002548956	Fludarabine	6.1	0.2	−9.8
NCP002408	F03	SAM001246877	Benzbromarone	5.2	1.6	−9.7
NCP002362	F02	SAM001246708	Nitazoxanide	11.1	0.5	−9.2
NCP002408	H07	SAM001247094	Rimcazole	6.7	3.4	−9.2
NCP002408	B04	SAM001246876	6-Azauridine	8.3	2.9	−9.1
NCP002295	H08	SAM001246989	Maprotiline hydrochloride	10.7	2.1	−9.1
Top candidates in 17Cl-1 cells						
NCP002408	C11	SAM001246822	Homoharringtonine	2.2	0.1	−10.2
NCP003132	C05	SAM002548956	Fludarabine	2.9	0.2	−10.1
NCP002954	B10	SAM002554903	Hexachlorophene	3.6	0.3	−10.0
NCP002353	G07	SAM001246553	Triptolide	3.7	0.3	−10.0
NCP002408	F03	SAM001246877	Benzbromarone	3.8	0.9	−10.0
NCP002408	H07	SAM001247094	Rimcazole	4.2	0.5	−10.0
NCP002353	F08	SAM001246770	Oxaprozin	4.5	0.3	−9.9
NCP003132	B04	SAM002699896	Mitoxantrone	7.6	2.0	−9.4
NCP002353	H06	SAM001246559	Epirubicin hydrochloride	9.0	1.2	−9.4
NCP002438	B02	SAM001246570	Vincristine sulfate	11.1	0.7	−9.2
NCP002322	F07	SAM001246679	Itraconazole	7.9	2.9	−9.2
NCP002362	B04	SAM001246780	VinorelbineÂ tartrate	7.6	3.2	−9.1
NCP002322	A06	SAM001246689	Docetaxel	12.2	1.0	−9.1
NCP002353	G02	SAM001246736	Carvedilol	12.6	0.9	−9.1

Note: Data showing here were obtained from validation study. Drug candidates are ranked from strongest to weakest antiviral efficacy according to SSMD score. Only the candidates with an SSMD score of less than −9 are listed. Mean, average luciferase activity of triplicate expressed as percentage of the control (DMSO), which is 100%. SD, standard deviation of the mean. SSMD, strictly standardized mean difference.

In an effort to identify potential drugs capable of inhibiting coronavirus infection, in the present study, we performed an in vitro screen of a small molecule library from the National Institutes of Health Clinical Collections (NCC). Because both SARS and MERS coronaviruses belong to the same biologically and genetically closely related *Betacoronavirus* subgroup as murine coronavirus, we used a recombinant murine coronavirus expressing a luciferase reporter gene as a safe surrogate to evaluate the anti-coronavirus efficacy of the drugs. Because preclinical and/or clinical data for these small molecules or compounds are already available, identification of potential antiviral candidates will allow us to rapidly advance the process for discovery and development of efficient anti-coronavirus drugs. Our screen identified 84 compounds with anti-coronavirus properties. Importantly, several compounds exhibited robust anti-coronavirus activity at micromolar or nanomolar concentrations, without overt cytotoxicity to host cells. Thus, these compounds can be advanced to animal and clinical trials, having the potential to be developed as effective anti-coronavirus drugs.

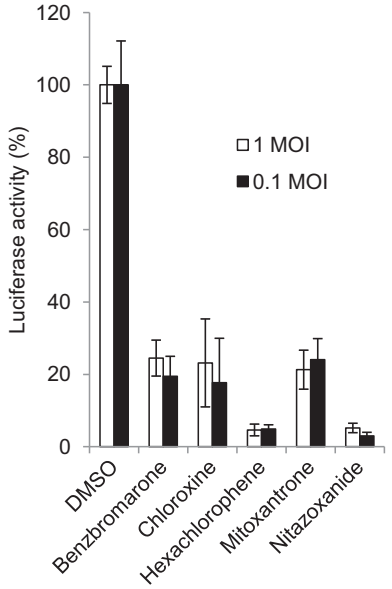

Fig. 1. Effect of candidate drugs on MHV infection at different MOIs. DBT cells were treated with drugs at 10 μM for 1 h and then infected with MHV-2aFLS at MOI of 1 or 0.1 in the presence of the indicated drugs for 8 h. Cells were then lysed for determining luciferase activity. Cells treated with 1% DMSO were served as control. The antiviral effectiveness of the drugs is expressed as percent luciferase activity to the control, which is 100%. Data represent mean of 3 independent treatments and standard deviation of the means.

2. Materials and methods

2.1. Cells, virus, and reagents

Mouse astrocytoma DBT and fibroblast 17Cl-1 cells were cultured at 37 °C in DMEM containing 10% fetal bovine serum (FBS), penicillin (100 units/ml), and streptomycin (100 μg/ml). A recombinant murine coronavirus mouse hepatitis virus (MHV) strain A59 expressing firefly luciferase, termed MHV-2aFLS (de Haan et al., 2003), was used for screening throughout the study. Wild-type MHV-A59, MHV-A59GFP (Das Sarma et al., 2002), MHV-1, MHV-2, and MHV-JHM were also used for some experiments. Virus titer was determined by standard plaque assay. Bovine coronavirus strain L9 (BCoV-L9) (Zhang et al., 1991), and human enteric coronavirus strain 4408 (HECoV-4408) (Zhang et al., 1994) were grown in human rectal tumor (HRT)-18 cells. Monoclonal antibody (mAb) J.3.3 was used for detecting MHV N protein, and mAb#46 for the N protein of BCoV-L9 and HECV-4408 (Zhang et al., 1994). Antibody to β-actin was purchased from Invitrogen. Goat anti-mouse

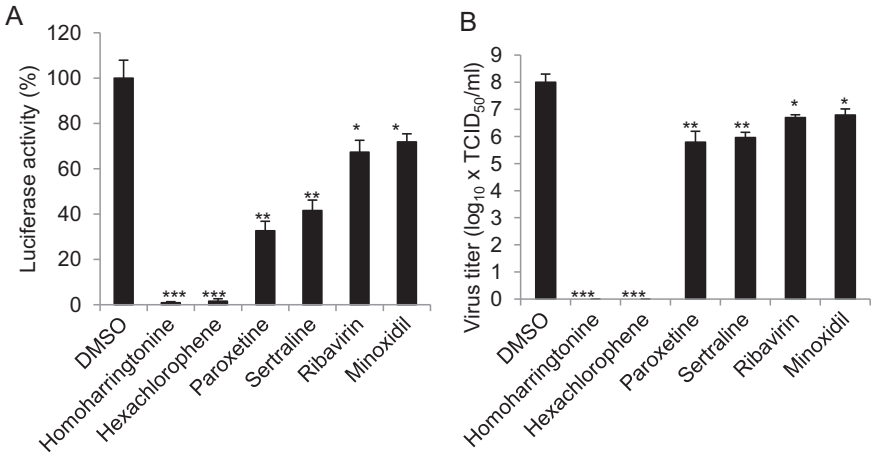

Fig. 2. Correlation of inhibition on luciferase reporter expression and virus titer. DBT cells were treated with various drugs as indicated (10 μM) or DMSO (1%) as a control for 1 h and then infected with MHV-2aFLS at MOI of 1 for 8 h. The medium was harvested for determining viral titer ($TCID_{50}$) (B) and cells were lysed for determining luciferase activity (A). Data indicate the mean of 3 replicates (independent treatments) and standard deviation of the mean. Statistical significance of the inhibitory effect of the drugs on luciferase activity (A) or virus titer (B) as compared to those of DMSO control is indicated by the number of asterisks ($^{*}p < 0.05$; $^{**}p < 0.01$; $^{***}p < 0.001$).

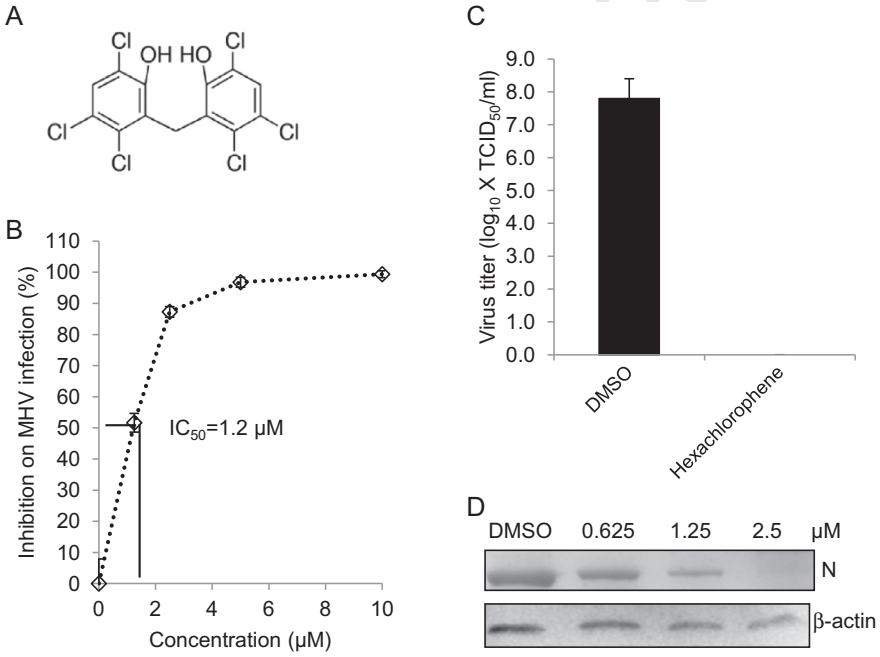

Fig. 3. Inhibitory effect of hexachlorophene on MHV infection. (A) Chemical structure of hexachlorophene. (B) Determination of IC_{50}. DBT cells were treated with hexachlorophene at various concentrations as indicated or 1% DMSO (vehicle control) for 1 h, and were infected with MHV-2aFLS at MOI of 1 in the presence of the drug for 8 h. Cells were then lysed for luciferase assay. Inhibition of MHV infection was expressed as percent reduction in luciferase activity following drug treatment compared to the control, and the IC_{50} was then calculated as indicated by the solid lines. (C) Inhibition of viral titer. DBT cells were treated with hexachlorophene (10 μM) or DMSO (1%) as a control for 1 h and then infected with MHV-2aFLS at MOI of 1 for 12 h. The medium was harvested for determining viral titer ($TCID_{50}$). Data indicate the mean of 3 replicates and standard deviation of the mean. (D) Inhibition of viral N protein expression. The experiments were performed identically to (C), except that different concentrations of the drugs were used. Following drug treatment and viral infection, cells were lysed to evaluate viral N protein expression levels by Western blotting. Beta-actin serves as a loading control.

IgG conjugated with horseradish peroxidase (HRP) or with FITC was purchased from Sigma–Aldrich.

2.2. Screening of small molecule drug library

The NCC library contains a total of 727 small molecule drugs (compounds) supplied in 96-well plates that are prepared in DMSO at 1 mM (http://www.nihclinicalcollection.com). For screening, 10 μl of each drug was first transferred to a new 96-well plate and diluted to 100 μl with Opti-MEM I serum-free medium to make stock plates. Then, 10 μl of the stock was transferred to a well in another 96-well plate and mixed with 90 μl of MHV-2aFLS in DMEM/TPB10 to give a final concentration of 10 μM for each drug. The drug/virus mixture (45 μl) was delivered to each well and the infection was carried out for 8 h. The vehicle control contained 1% DMSO. For primary screening, duplicate plates were used. For validation screening, experiments were conducted in triplicate plates. At the end of the infection, culture medium was removed and cells were stored at −80 °C overnight. The plates were then allowed to thaw at room temperature and 50 μl of

luciferase reagent was added to each well followed by gentle shaking for 10 min. The luciferase activity was determined using a Synergy 2 microplate reader with Gen 5 software (Biotek). Data were exported into Excel files for statistical analysis.

2.3. Cell viability assay

Cells grown in 96-well plates were incubated for 16 h with each drug at 10 μM and then cell viability was determined using the XTT assay kit TOX2-1KT according to the manufacturer's instruction (Sigma–Aldrich). DMSO at 1% served as vehicle control.

2.4. Western blot analysis and immunofluorescence assay (IFA)

For detecting proteins, either Western blot analysis or IFA was performed as previously described (Cao and Zhang, 2012).

2.5. Determination of virus titer ($TCID_{50}$)

Virus titer was determined by the standard 50% tissue culture infectious dose ($TCID_{50}$) in DBT cells in a 96-well plate.

2.6. Statistics analysis

Luciferase data from each library screening plate were combined and used for statistical analysis. Mean luciferase activity for replicates and standard deviation (SD) of the mean were calculated by standard statistics methods and were expressed as a percentage of the negative control (DMSO), which was set as 100%. Student's *t*-test was used to calculate *p*-values for statistical significance. Strictly standardized mean difference (SSMD) (Zhang, 2007) was used to select the candidates with a score of −2 or less for inhibitors.

3. Results

3.1. Screening of the NCC drug library for anti-coronavirus activity

Primary screening of the entire NCC library was performed in DBT cells infected with MHV-2aFLS. Duplicate plates were used for the screening and SSMD was used for hit selection and ranking. Recently, SSMD has been widely used for hit selection in high-throughput screening assay (HTS) such as siRNA and small molecule screenings as well as antiviral drug selection (Andruska et al., 2012; Aulner et al., 2013; Gough et al., 2014; Rachidi et al., 2014; Zhang, 2007). A negative value of SSMD suggests inhibitory effect while a positive value indicates enhanced effect of the compound. An SSMD score of <−2 suggests strong inhibitory effect (Zhang, 2007). Thus, we used this score as a cut-off threshold for hit selection. Results showed that 84 drugs had an SSMD score of less than −2, indicating that these drugs likely have anti-MHV activities. Of the 84 drug candidates, 37 exhibited very strong inhibition of MHV infection with an SSMD score of <−5 (Supplemental Table 1). All candidate anti-coronavirus drugs were subjected to further validation (see below).

3.2. Validation of the candidate drugs

To verify the antiviral effect of the candidate drugs, secondary screening was carried out in both DBT and 17Cl-1 cells. We found that 70 and 69 of the 84 drugs, respectively, inhibited MHV infection in DBT and 17Cl-1 cells (Supplemental Table 1). Specifically, in DBT cells, 11 drugs strongly inhibited viral infection with an SSMD score of less than −9 (Table 1). In 17Cl-1 cells, viral infection was strongly inhibited by 14 drugs, which exhibited SSMD scores of less than −9 (Table 1). Cell viability assays revealed that all the candidate drugs did not significantly decrease cell viability at the

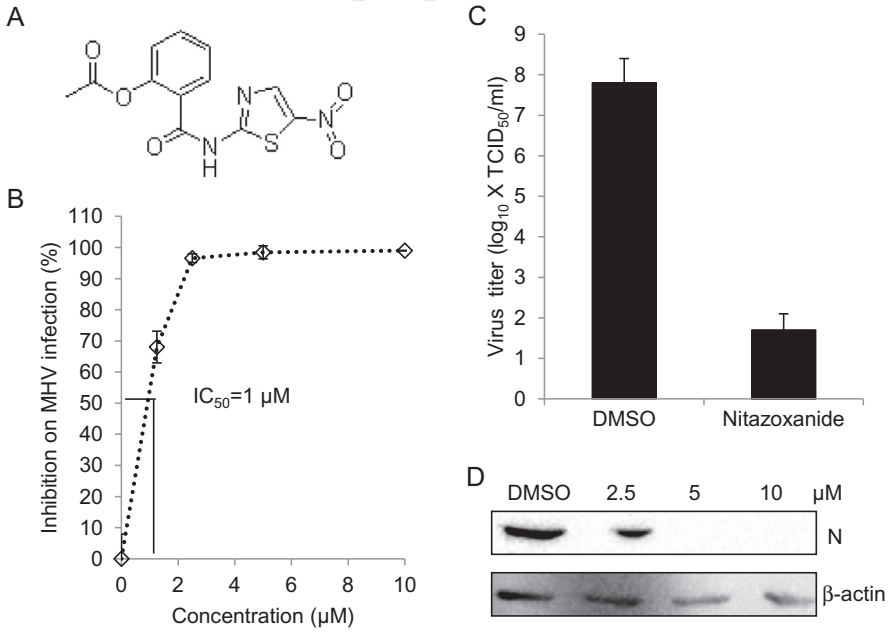

Fig. 4. Inhibitory effect of nitazoxanide on MHV infection. (A) Chemical structure of nitazoxanide. (B) Determination of IC_{50}. DBT cells were treated with nitazoxanide at various concentrations or 1% DMSO (vehicle control) for 1 h, and were infected with MHV-2aFLS at MOI of 1 in the presence of the drug for 8 h. Cells were then lysed for luciferase assay. Inhibition of drug on MHV infection was expressed as percent reduction on luciferase activity to the control and the IC_{50} was then calculated as indicated by the solid lines. (C) Inhibition of viral titer. DBT cells were treated with nitazoxanide (10 μM) or DMSO (1%) as a control for 1 h and then infected with MHV-2aFLS at MOI of 1 for 12 h. The medium was harvested for determining viral titer ($TCID_{50}$). Data indicate the mean of 3 replicates and standard deviation of the mean. (D) Inhibition of viral N protein expression. The experiments were performed identically to (C), except that different concentrations of the drugs were used. Following drug treatment and viral infection, cells were lysed to evaluate viral N protein expression levels by Western blotting. Beta-actin serves as a loading control.

Please cite this article in press as: Cao, J., et al. A screen of the NIH Clinical Collection small molecule library identifies potential anti-coronavirus drugs. Antiviral Res. (2014), http://dx.doi.org/10.1016/j.antiviral.2014.11.010

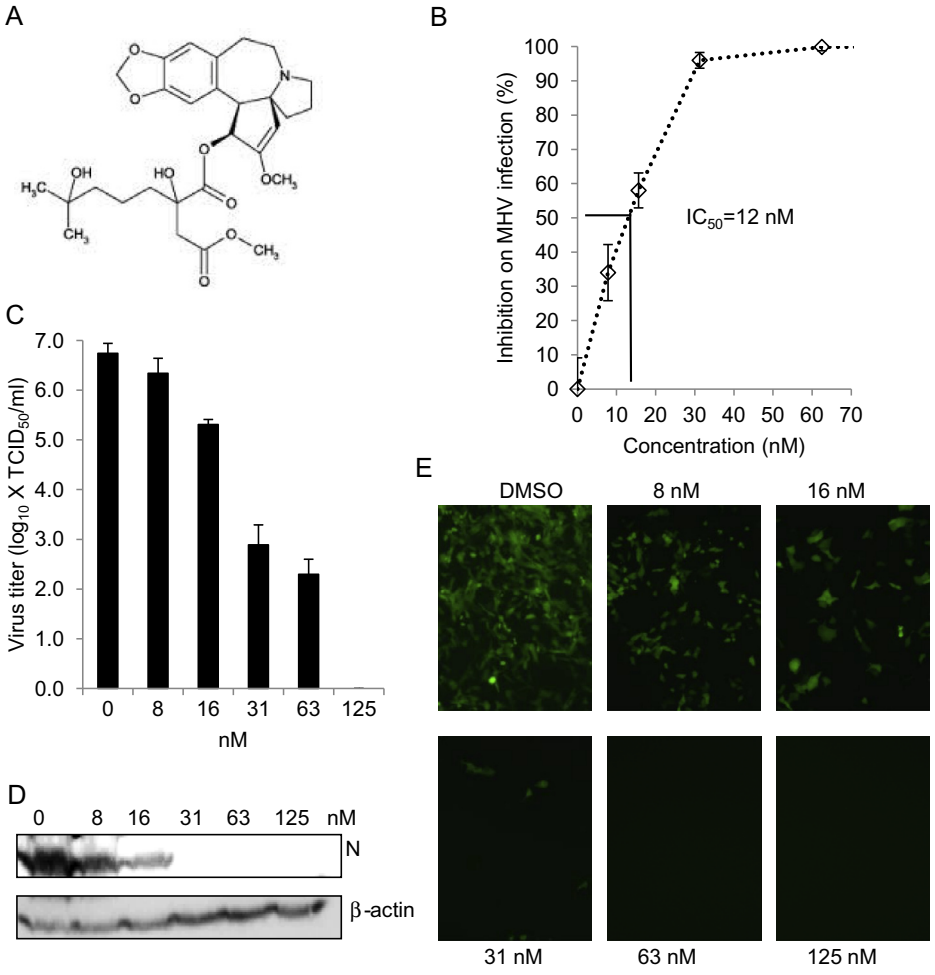

Fig. 5. Inhibitory effect of homoharringtonine on MHV infection. (A) Chemical structure of homoharringtonine. (B) Determination of IC_{50}. DBT cells were treated with homoharringtonine at various concentrations or 1% DMSO (vehicle control) for 1 h, and were infected with MHV-2aFLS at MOI of 1 in the presence of the drug for 8 h. Cells were then lysed for luciferase assay. Inhibition of drug on MHV infection was expressed as percent reduction on luciferase activity to the control and the IC_{50} was then calculated as indicated by the solid lines. (C–E) Cells were pretreated with homoharringtonine at various concentrations as indicated or 1% DMSO for 1 h. Cells were then infected with MHV-A59 for 12 h (C and D in DBT cells) or MHV-A59GFP for 16 h (E in 17Cl-1 cells) at MOI of 1 in the presence of the drug. (C) Virus titer in the medium was determined by $TCID_{50}$. Data represent the mean of 3 replicates and standard deviation of the mean. (D) Viral N protein expression in cell lysates was detected by Western blotting using mAb J.3.3. Beta-actin serves as a loading control. (E) Expression of GFP was directly observed using a fluorescence microscope (Olympus IX-70), and images were captured using a digital camera (Zeiss).

concentrations tested (Supplemental Table 2). Comparative analysis revealed that 10 candidate drugs exhibited antiviral effects only in DBT cells, indicating that some differential cellular targets may play a role in viral infection (Supplemental Table 1). Importantly, 61 of the candidate drugs were commonly effective in inhibiting viral infection of both DBT and 17Cl-1 cells (Supplemental Table 1), suggesting that the cellular targets for these drugs are conserved between the two cell types. Interestingly, many of the anti-coronavirus candidate drugs could be grouped by clinical application. The 3 most abundant groups of anti-coronavirus candidate drugs are those used for cancer treatment or as antidepressant and antipsychotic (Supplemental Table 3).

To evaluate whether different MOIs would impact the outcome of our screen, DBT cells were treated with one of the 5 drugs (benzbromarone, chloroxine, hexachlorophene, mitoxantrone, and nitazoxanide) or DMSO for 1 h and then infected with MHV-2aFLS at MOIs of 1 or 0.1 for 8 h in the presence of the respective drugs. As shown in Fig. 1, when compared with vehicle (DMSO) control, the reduction in luciferase activity was similar at both MOIs, indicating that the inhibitory effect of these candidate drugs on MHV infection was independent of MOI.

To validate the statistical approach employed for identifying candidate drugs, we selected two representative drugs from each of the three groups based on their SSMD score (low, median, and high), and determined their inhibitory effects on virus infection. Indeed, two drugs (homoharringtonine and hexachlorophene) with the lowest SSMD score (≈−10) almost completely inhibited coronavirus infection (a reduction of >95% in luciferase activity and $\geqslant 8\log_{10}$ in virus titer) while ribavirin and Minoxidil with the highest SSMD score (>−2) had the least inhibitory effect on virus infection (a reduction of ≈30% in luciferase activity and $\approx 1\log_{10}$ in virus titer); the other two drugs (Paroxetine and Sertraline) with a median SSMD score (≈−5) reduced luciferase activity by about 50% and virus titer about $2\log_{10}$ (Fig. 2). Thus, the inhibitory effect of the drugs correlated inversely and proportionally with the SSMD score. These data demonstrate a general applicability of the SSMD scoring system for selecting candidate drugs (Zhang, 2007).

To further confirm the anti-coronavirus activity of the candidate drugs, we selected 3 top-ranked drugs for additional studies. First, we determined the IC_{50}. DBT cells were infected with MHV-2aFLS at MOI of 1, and then treated with hexachlorophene, nitazoxanide, and homoharringtonine (panel A in Figs. 3–5) at various

Please cite this article in press as: Cao, J., et al. A screen of the NIH Clinical Collection small molecule library identifies potential anti-coronavirus drugs. Antiviral Res. (2014), http://dx.doi.org/10.1016/j.antiviral.2014.11.010

concentrations. Results showed that while the IC_{50} varied widely from about 11 nM for homoharringtonine to about 1 μM for hexachlorophene and nitazoxanide, the antiviral effect for each drug was clearly dose-dependent (panel B in Figs. 3–5).

As complementary alternative approaches to luciferase reporter assays, we also performed $TCID_{50}$ and Western blot. DBT cells were treated with the 3 drugs at indicated concentrations for 1 h and then infected with MHV-2aFLS at MOI of 1. At 12 h p.i., viral titer in the medium was determined by $TCID_{50}$ and viral N protein in the cells was assessed by Western blot. As expected from the luciferase reporter screen, all 3 drugs had a robust inhibitory effect on virus titer (a reduction of $\geqslant 8 \log_{10}$ for hexachlorophene and homoharringtonine (Figs. 2B, 3C and 5C) and $>6 \log_{10}$ for nitazoxanide (Fig. 4C)). Consistent with the inhibition of virus production, viral N protein expression was undetectable following treatment with hexachlorophene at 2.5 μM, nitazoxanide at 5 μM and homoharringtonine at 31 nM (panel D in Figs. 3–5). A dose-dependent inhibition of viral N protein and EGFP reporter gene expression was also evident (panel D in Figs. 3–5 and Fig. 5E). Although there were slight variations in viral inhibition measured by the 3 methods (compare data in Supplemental Table 1 with those in Figs. 3–5), the overall inhibitory effect of the selected drugs on MHV infection can be firmly established.

3.3. Identification of candidate drugs that exert anti-coronavirus effect at different stages of the virus life cycle

To gain insight into steps in the virus life cycle targeted by candidate drugs, we sought to define whether candidate drugs were inhibitory when administered before or after infection of host cells. Since the original screen involved simultaneously treating and infecting target cells, we evaluated post-entry effects by treating cells with the 70 candidate drugs identified from the previous screenings at 3 h p.i. for 5 h, and determined luciferase activity at 8 h p.i. Results showed that 19 of the drugs significantly reduced luciferase activity (SSMD < −2), 9 of which (homoharringtonine, duloxetine, chloroxine, hexachlorophene, ebselen, nitazoxanide, mitoxantrone, disulfiram, and 6-azauridine) had an SSMD score of less than −9 (Supplemental Table 4). It is important to note that even the well-known anti-RNA virus inhibitor ribavirin in the library had only a relatively weak inhibitory effect on MHV replication with an SSMD score of −1.7 and a reduction of virus titer of $\approx 1 \log_{10}$ (see Supplemental Table 1 and Fig. 2), which suggests that several of the drugs identified here may be more potent than ribavirin. To further corroborate these findings, in a second set of experiments, cells were treated with 11 selected drugs at 1 h prior to, or 3 h after, virus infection. It was found that all 11 drugs strongly inhibited luciferase activity at either time point (Fig. 6A). In agreement with results obtained using the luciferase reporter virus, EGFP expression from MHV-A59GFP also was drastically inhibited when the drugs were added at 3 h p.i. (Fig. 6B; further data not shown). These data indicate that these drugs inhibited virus infection at post entry stages (most likely at the step of viral replication), because most, if not all, infectious viral particles have entered into cells during the first 3 h of infection, with MHV biosynthesis commencing by 1 h p.i. in DBT cells (Zhu et al., 2009). In contrast, 51 other drugs did not inhibit luciferase activity (SSMD > −2) when the drugs were added 3 h p.i. (Supplemental Table 5). This indicates that these drugs most likely blocked viral entry only, because their antiviral activity was established during primary and secondary screenings when drug treatment and virus infection were carried out at the same time. To further support this conclusion, cells were treated with selected candidate drugs at either 1 h before, or 3 h after, virus infection and luciferase activity was determined at 8 h p.i. As expected, all 7 candidate drugs inhibited luciferase activity by more than 50% when the

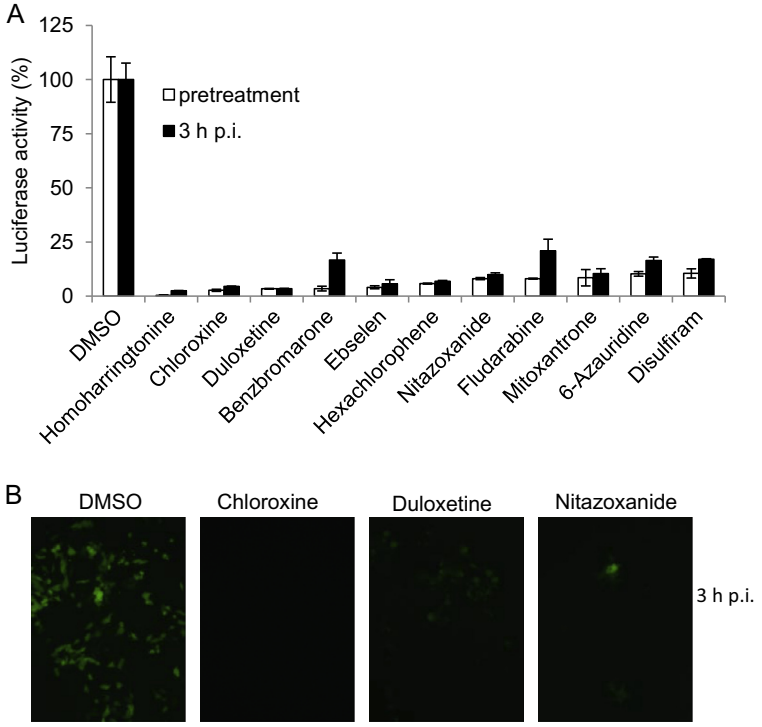

Fig. 6. Identification of candidate drugs that inhibit MHV infection during viral replication. (A) DBT cells were either treated with drugs (10 μm) as indicated or DMSO (1%) at 1 h before or 3 h after infection with MHV-2afls at MOI of 1. The cells were lysed at 8 h p.i. and luciferase activity was measured and expressed as a percentage of DMSO control. Data represent the mean of triplicate experiments and standard deviation from the mean. (B) 17Cl-1 cells were either treated with drugs (10 μm) as indicated or DMSO (1%) At 1 h before or 3 h after infection with MHV-A59GFP at MOI of 1. At 16 h p.i. EGFP expression was observed using a fluorescence microscope (Olympus IX-70), and images were captured using a digital camera (Zeiss). Representative images for 3 h post infection are shown.

Please cite this article in press as: Cao, J., et al. A screen of the NIH Clinical Collection small molecule library identifies potential anti-coronavirus drugs. Antiviral Res. (2014), http://dx.doi.org/10.1016/j.antiviral.2014.11.010

drugs were added 1 h before infection but had no inhibitory effect when added at 3 h p.i. (Fig. 7A). Interestingly, some of the drugs (clomid, oxaprozin, and azathioprine) instead enhanced luciferase activity when added at 3 h p.i. The reason for this enhancement is not currently clear. Consistent with the results from luciferase assay, viral gene expression as measured by EGFP reporter expression was strongly inhibited only when the drugs were added 1 h prior to infection (Fig. 7B).

3.4. Potential broad-spectrum anti-coronavirus activity of candidate drugs

To extend our findings from MHV strain A59, we utilized several different MHV strains, which possess various pathogenic phenotypes in cell culture and animals. For example, JHM strain causes more extensive cell fusion in DBT cell and more severe encephalitis and demyelination in mice than does A59 strain, while MHV-2 does not induce cell fusion or cause encephalitis/demyelination in mice (Das Sarma et al., 2000; Hirano et al., 1974; Phillips et al., 1999). Thus, DBT cells were treated with homoharringtonine at 60 nM for 1 h, and then infected with MHV-1, MHV-2, and MHV-JHM at MOI of 1 for 12 h. Viral N protein was then detected by Western blot. As shown in Fig. 8A, the N protein for all 3 MHV strains was undetectable in the presence of the drugs, while in control untreated samples, expression of the N protein was robust. These data suggest that homoharringtonine is capable of inhibiting infection by various MHV strains. Furthermore, treatment of human HRT-18 cells with homoharringtonine or hexachlorophene prior to infection with bovine coronavirus (BCoV-L9) or human enteric coronavirus (HECoV-4408) also resulted in potent inhibition of viral N protein expression as judged by immunofluorescence analysis (Fig. 8B and C). Thus, by extrapolating from these results, we postulate that a great number of candidate anti-coronavirus drugs identified through our screen of the NCC library likely have broad antiviral activity against both human and animal coronaviruses.

4. Discussion

In this study we have identified a substantial number of candidate drugs that exhibited anti-coronavirus activity. It is worth noting that some of the same candidate drugs identified in this study have been previously shown to inhibit infections by other viruses. For example, nitazoxanide was initially discovered to have anti-protozoal activity (White, 2003), but it also inhibits infection by Influenza A virus (Rossignol et al., 2009), hepatitis B virus (HBV) (Korba et al., 2008), hepatitis C virus (Keeffe and Rossignol, 2009), Japanese encephalitis virus (Shi et al., 2014), and Norovirus

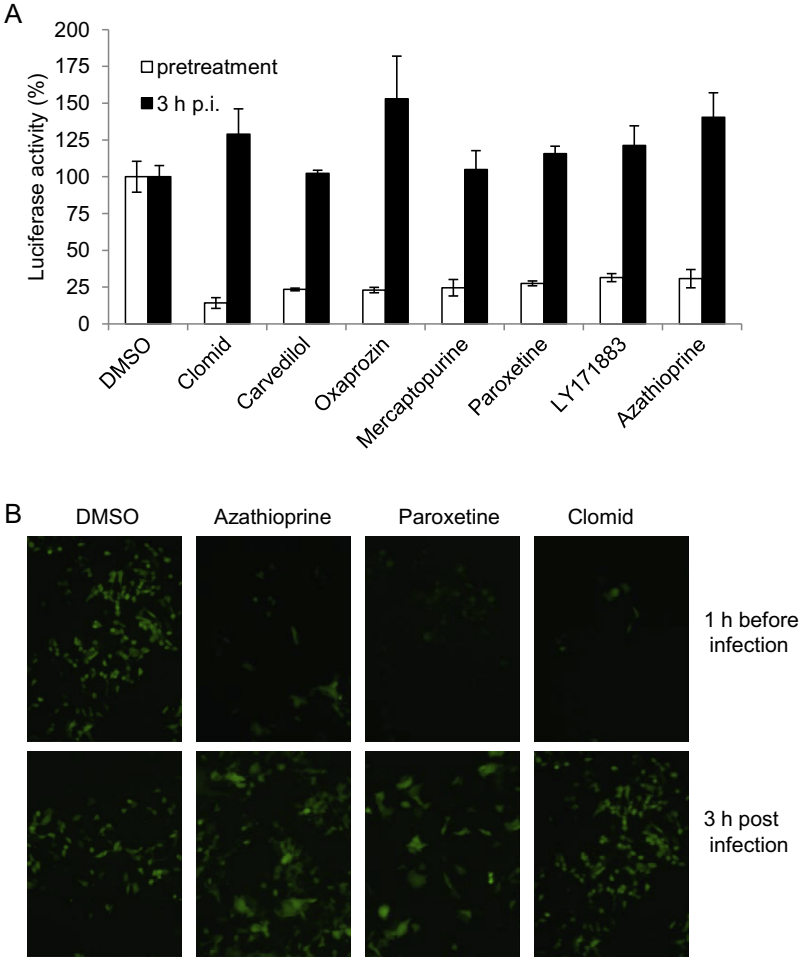

Fig. 7. Identification of candidate drugs that inhibit MHV infection during cell entry. (A) DBT cells were either treated with drugs (10 μM) as indicated or DMSO (1%) at 1 h before or 3 h after infection with MHV-2aFLS at MOI of 1. The cells were lysed at 8 h p.i. and luciferase activity was measured and expressed as a percentage of DMSO control. Data represent the mean of triplicate experiments and standard deviation from the mean. (B) 17Cl-1 cells were either treated with drugs (10 μM) as indicated or DMSO (1%) at 1 h before or 3 h after infection with MHV-A59GFP at MOI of 1. At 16 h p.i. EGFP expression was observed using a fluorescence microscope (Olympus IX-70), and images were captured using a digital camera (Zeiss).

Please cite this article in press as: Cao, J., et al. A screen of the NIH Clinical Collection small molecule library identifies potential anti-coronavirus drugs. Antiviral Res. (2014), http://dx.doi.org/10.1016/j.antiviral.2014.11.010

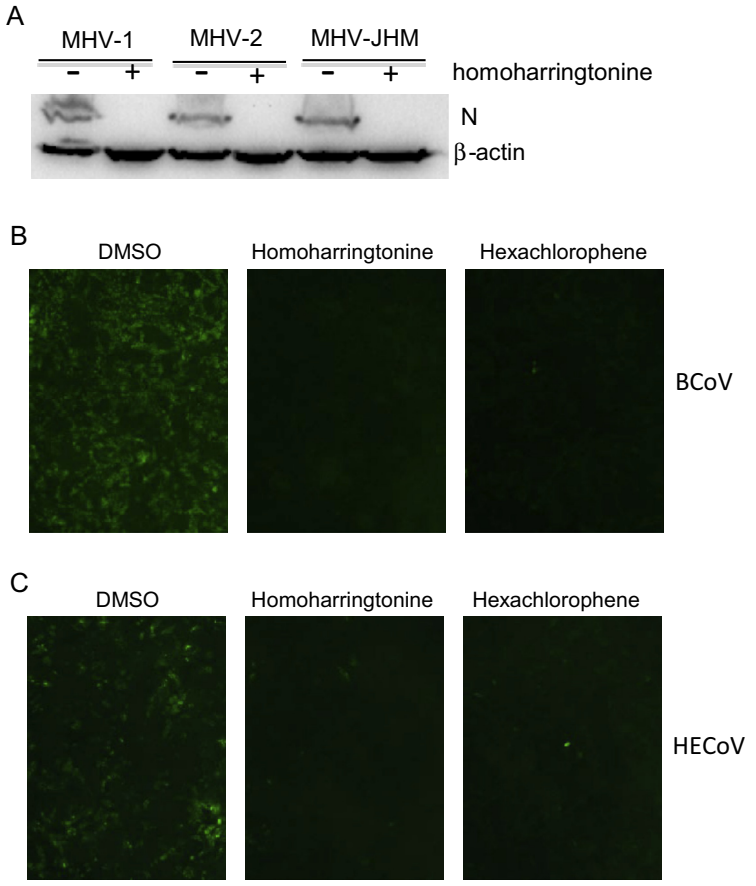

Fig. 8. Candidate drugs are capable of inhibiting infection with diverse coronaviruses. (A) DBT cells were infected with various MHV strains (MHV-1, MHV-2, and MHV-JHM) in the presence of the indicated drugs for 12 h, and the viral N protein was detected by Western blot using mAb J.3.3. Beta-actin serves as loading control. (B and C) HRT-18 cells were infected with either BCoV-L9 (B) or HECoV-4408 (C) in the presence of the drugs for 36 h, and the viral N protein was detected by IFA using specific mAb#46. The concentration of homoharringtonine is 1 μM and hexachlorophene is 5 μM. The control is 1% DMSO.

(Siddiq et al., 2011). Hexachlorophene was widely used as a disinfectant, and it is very useful as a topical anti-infective and anti-bacterial agent. At 0.75%, hexachlorophene is effective in inactivation of rotavirus (Sattar et al., 1983), and at 10 μM, it inhibited SARS-CoV replication in Vero cells (Hsu et al., 2004). A recent report demonstrated that hexachlorophene inhibited both BK polyomavirus and Simian Virus 40 infection by inhibiting the ATPase activity of large T antigen (Seguin et al., 2012). Benzbromarone is a non-competitive inhibitor of xanthine oxidase (Sinclair and Fox, 1975), a very potent inhibitor of CYP2C9 (Hummel et al., 2005), and was used for treatment of gout (Reinders et al., 2009). Benzbromarone also inhibits influenza virus infection by binding to PA protein and decreasing viral RNA polymerase activity (Fukuoka et al., 2012). 6-azauridine is a pyrimidine analog that can inhibit diverse viruses by inhibiting viral RNA synthesis. Viruses inhibited by 6-azauridine include another human coronavirus HCoV-NL63 (Pyrc et al., 2006), avian coronavirus infectious bronchitis virus (Barlough and Shacklett, 1994), foot-and-mouth disease virus (Kim et al., 2012), tick-borne flaviviruses such as Kyasanur Forest disease virus, Alkhurma hemorrhagic fever virus and Omsk hemorrhagic fever virus (Crance et al., 2003; Flint et al., 2014), and West Nile virus (Morrey et al., 2002). Homoharringtonine, an inhibitor of translation elongation, also inhibits HBV infection in vitro (Romero et al., 2007). Of particular note is the finding from this study that homoharringtonine is the strongest inhibitor against various coronaviruses with the lowest IC_{50}. Other inhibitors such as itraconazole, albendazole, nelfinavir mesylate, and artesunate inhibit HIV-1 infection (de Gans et al., 1992; Efferth et al., 2008; Tebas and Powderly, 2000; Walson et al., 2008) and tetraethylthiuram disulfide can inhibit respiratory syncytia virus, Semliki Forest virus, and vesicular stomatitis virus (Boukhvalova et al., 2010). These data suggest that some of the candidate drugs exhibit broad-spectrum antiviral activity.

The overall hit rate for the library screen is approximately 10%. This rate is indeed very high compared to previous screens of raw chemical libraries. However, the high hit rate is not particularly surprising, considering that the NCC library is a collection of drugs that have undergone multiple selections (screens) from numerous different libraries. Collected in the library are only those that have exhibited potent biologic activities against various diseases and that have advanced from pre-clinical to clinical trials. Thus, the NCC library consists primarily of screen "winners". Another possible explanation for the high hit rate is that clusters of the drugs that are selected may target the same cellular pathways (see Supplemental Table 3) that are critical for coronavirus infection. On the other hand, the SSMD scoring system is more stringent than the traditional method of using 2 SD (standard deviation) cut-off. As a result, those drugs that have a weak antiviral activity are not selected in the current screen, as in the case of ribavirin, a well-known anti-RNA virus drug (SSMD = −1.7; a reduction of ≈1 $\log_{10}$ in virus titer) (Supplemental Table 1 and Fig. 2). Thus, the high hit rate is not likely due to utilization of the more stringent SSMD scoring system.

In summary, identification of candidate anti-coronavirus drugs from the NCC library in the current study will advance the discovery and development process, thereby allowing us to focus on a

Please cite this article in press as: Cao, J., et al. A screen of the NIH Clinical Collection small molecule library identifies potential anti-coronavirus drugs. Antiviral Res. (2014), http://dx.doi.org/10.1016/j.antiviral.2014.11.010

few potent inhibitors to rapidly prioritize for preclinical and clinical trials. This is particularly urgent as the newly emergent MERS-CoV continues to spread from the Middle East to the rest of the world.

5. Conclusion

Of the 727 small molecules in the NCC drug library screened, 84 were found to have a significant anti-coronavirus effect, of which 51 blocked virus entry while 19 others inhibited viral replication. Several candidate drugs exhibited robust antiviral activity against human and diverse animal coronaviruses at micromolar or nanomolar concentrations without any cytotoxicity.

Acknowledgments

We thank Drs. P. Rottier and C. de Haan (Utrecht University, The Netherlands) for kindly providing the recombinant MHV-2aFLS. We also thank James A. Stahl (UAMS) for his technical assistance.

This work was supported by funds from the Department of Microbiology and Immunology, UAMS to XZ, start-up funds from the UAMS College of Medicine and Arkansas Biosciences Institute to Jiren Charity Foundation.

Appendix A. Supplementary data

Supplementary data associated with this article can be found, in the online version, at http://dx.doi.org/10.1016/j.antiviral.2014.11.010.

References

Al-Tawfiq, J.A., Momattin, H., Dib, J., Memish, Z.A., 2014. Ribavirin and interferon therapy in patients infected with the Middle East respiratory syndrome coronavirus: an observational study. Int. J. Infect. Dis. 20, 42–46.

Andruska, N., Mao, C., Cherian, M., Zhang, C., Shapiro, D.J., 2012. Evaluation of a luciferase-based reporter assay as a screen for inhibitors of estrogen-ERalpha-induced proliferation of breast cancer cells. J. Biomol. Screen. 17, 921–932.

Aulner, N., Danckaert, A., Rouault-Hardoin, E., Desrivot, J., Helynck, O., Commere, P.H., Munier-Lehmann, H., Spath, G.F., Shorte, S.L., Milon, G., Prina, E., 2013. High content analysis of primary macrophages hosting proliferating *Leishmania* amastigotes: application to anti-leishmanial drug discovery. PLoS Negl. Trop. Dis. 7, E2154.

Barlough, J.E., Shacklett, B.L., 1994. Antiviral studies of feline infectious peritonitis virus in vitro. Vet. Rec. 135, 177–179.

Boukhvalova, M.S., Prince, G.A., Blanco, J.C., 2010. Inactivation of respiratory syncytial virus by zinc finger reactive compounds. Virol. J. 7, 20.

Cao, J., Zhang, X., 2012. Comparative in vivo analysis of the nsp15 endoribonuclease of murine, porcine and severe acute respiratory syndrome coronaviruses. Virus Res. 167, 247–258.

Caul, E.O., Egglestone, S.I., 1977. Further studies on human enteric coronaviruses. Arch Virol. 54, 107–117.

CDC, 2004. SARS Basics Fact Sheet.

Crance, J.M., Scaramozzino, N., Jouan, A., Garin, D., 2003. Interferon, ribavirin, 6-azauridine and glycyrrhizin: antiviral compounds active against pathogenic flaviviruses. Antiviral Res. 58, 73–79.

Das Sarma, J., Fu, L., Tsai, J.C., Weiss, S.R., Lavi, E., 2000. Demyelination determinants map to the spike glycoprotein gene of coronavirus mouse hepatitis virus. J. Virol. 74, 9206–9213.

Das Sarma, J., Scheen, E., Seo, S.H., Koval, M., Weiss, S.R., 2002. Enhanced green fluorescent protein expression may be used to monitor murine coronavirus spread in vitro and in the mouse central nervous system. J. Neurovirol. 8, 381–391.

De Gans, J., Portegies, P., Tiessens, G., Eeftinck Schattenkerk, J.K., Van Boxtel, C.J., Van Ketel, R.J., Stam, J., 1992. Itraconazole compared with amphotericin B plus flucytosine in AIDS patients with cryptococcal meningitis. AIDS 6, 185–190.

De Haan, C.A., Van, G.L., Stoop, J.N., Volders, H., Rottier, P.J., 2003. Coronaviruses as vectors: position dependence of foreign gene expression. J. Virol. 77, 11312–11323.

De La Hamaide, S., 2014. Deadly pig virus likely to ease in us by year-end. <http://www.reuters.com/article/2014/05/20/us-pork-oie-idUSKBN0E01V920140520>.

Drosten, C., Gunther, S., Preiser, W., Van Der Werf, S., Brodt, H.R., Becker, S., Rabenau, H., Panning, M., Kolesnikova, L., Fouchier, R.A., Berger, A., Burguiere, A.M., Cinatl, J., Eickmann, M., Escriou, N., Grywna, K., Kramme, S., Manuguerra, J.C., Muller, S., Rickerts, V., Sturmer, M., Vieth, S., Klenk, H.D., Osterhaus, A.D., Schmitz, Doerr, H.W., . Identification of a novel coronavirus in patients with severe acute respiratory syndrome. N. Engl. J. Med. 348, 1967–1976.

Efferth, T., Romero, M.R., Wolf, D.G., Stamminger, T., Marin, J.J., Marschall, M., 2008. The antiviral activities of artemisinin and artesunate. Clin. Infect. Dis. 47, 804–811.

Falzarano, D. et al., 2013. Inhibition of novel beta coronavirus replication by a combination of interferon-alpha2b and ribavirin. Sci. Rep. 3, 1686.

Fan, H. et al., 2005. The nucleocapsid protein of coronavirus infectious bronchitis virus: crystal structure of its N-terminal domain and multimerization properties. Structure 13 (12), 1859–1868.

Flint, M., Mcmullan, L.K., Dodd, K.A., Bird, B.H., Khristova, M.L., Nichol, S.T., Spiropoulou, C.F., 2014. Inhibitors of the tick-borne, hemorrhagic fever-associated flaviviruses. Antimicrob. Agents Chemother. 58, 3206–3216.

Fukuoka, M., Minakuchi, M., Kawaguchi, A., Nagata, K., Kamatari, Y.O., Kuwata, K., 2012. Structure-based discovery of anti-influenza virus a compounds among medicines. Biochim. Biophys. Acta 1820, 90–95.

Gough, A.H., Chen, N., Shun, T.Y., Lezon, T.R., Boltz, R.C., Reese, C.E., Wagner, J., Vernetti, L.A., Grandis, J.R., Lee, A.V., Stern, A.M., Schurdak, M.E., Taylor, D.L., 2014. Identifying and quantifying heterogeneity in high content analysis: application of heterogeneity indices to drug discovery. PLoS One 9, E102678.

Hirano, N., Fujiwara, K., Hino, S., Matumoto, M., 1974. Replication and plaque formation of mouse hepatitis virus (MHV-2) in mouse cell line DBT culture. Arch. Gesamte Virusforsch. 44, 298–302.

Hsu, J.T., Kuo, C.J., Hsieh, H.P., Wang, Y.C., Huang, K.K., Lin, C.P., Huang, P.F., Chen, X., Liang, P.H., 2004. Evaluation of metal-conjugated compounds as inhibitors of 3CL protease of SARS-CoV. FEBS Lett. 574, 116–120.

Hummel, M.A., Locuson, C.W., Gannett, P.M., Rock, D.A., Mosher, C.M., Rettie, A.E., Tracy, T.S., 2005. CYP2C9 genotype-dependent effects on in vitro drug–drug interactions: switching of benzbromarone effect from inhibition to activation in the CYP2C9.3 variant. Mol. Pharmacol. 68, 644–651.

Jayaram, H. et al., 2006. X-ray structures of the N- and C-terminal domains of a coronavirus nucleocapsid protein: implications for nucleocapsid formation. J. Virol. 80 (13), 6612–6620.

Keeffe, E.B., Rossignol, J.F., 2009. Treatment of chronic viral hepatitis with nitazoxanide and second generation thiazolides. World J. Gastroenterol. 15, 1805–1808.

Kim, S.M., Park, J.H., Lee, K.N., Kim, S.K., Ko, Y.J., Lee, H.S., Cho, I.S., 2012. Enhanced inhibition of foot-and-mouth disease virus by combinations of porcine interferon-alpha and antiviral agents. Antiviral Res. 96, 213–220.

Korba, B.E., Montero, A.B., Farrar, K., Gaye, K., Mukerjee, S., Ayers, M.S., Rossignol, J.F., 2008. Nitazoxanide, tizoxanide and other thiazolides are potent inhibitors of hepatitis B virus and hepatitis C virus replication. Antiviral Res. 77, 56–63.

Ksiazek, T.G., Erdman, D., Goldsmith, C.S., Zaki, S.R., Peret, T., Emery, S., Tong, S., Urbani, C., Comer, J.A., Lim, W., Rollin, P.E., Dowell, S.F., Ling, A.E., Humphrey, C.D., Shieh, W.J., Guarner, J., Paddock, C.D., Rota, P., Fields, B., Derisi, J., Yang, J.Y., Cox, N., Hughes, J.M., Leduc, J.W., Bellini, W.J., Anderson, L.J., 2003. A novel coronavirus associated with severe acute respiratory syndrome. N. Engl. J. Med. 348, 1953–1966.

Lim, P.L., Lee, T.H., Rowe, E.K., 2013. Middle East respiratory syndrome coronavirus (MERS CoV): update 2013. Curr. Infect. Dis. Rep. 15, 295–298.

Marra, M.A., Jones, S.J., Astell, C.R., Holt, R.A., Brooks-Wilson, A., Butterfield, Y.S., Khattra, J., Asano, J.K., Barber, S.A., Chan, S.Y., Cloutier, A., Coughlin, S.M., Freeman, D., Girn, N., Griffith, O.L., Leach, S.R., Mayo, M., Mcdonald, H., Montgomery, S.B., Pandoh, P.K., Petrescu, A.S., Robertson, A.G., Schein, J.E., Siddiqui, A., Smailus, D.E., Stott, J.M., Yang, G.S., Plummer, F., Andonov, A., Artsob, H., Bastien, N., Bernard, K., Booth, T.F., Bowness, D., Czub, M., Drebot, M., Fernando, L., Flick, R., Garbutt, M., Gray, M., Grolla, A., Jones, S., Feldmann, H., Meyers, A., Kabani, A., Li, Y., Normand, S., Stroher, U., Tipples, G.A., Tyler, S., Vogrig, R., Ward, D., Watson, B., Brunham, R.C., Krajden, M., Petric, M., Skowronski, D.M., Upton, C., Roper, R.L., 2003. The genome sequence of the SARS-associated coronavirus. Science 300, 1399–1404.

Mitka, M., 2013. Deadly MERS coronavirus not yet a global concern. JAMA 310, 569.

Morrey, J.D., Smee, D.F., Sidwell, R.W., Tseng, C., 2002. Identification of active antiviral compounds against a New York isolate of West Nile virus. Antiviral Res. 55, 107–116.

Phillips, J.J., Chua, M.M., Lavi, E., Weiss, S.R., 1999. Pathogenesis of chimeric MHV4/MHV-A59 recombinant viruses: the murine coronavirus spike protein is a major determinant of neurovirulence. J. Virol. 73, 7752–7760.

Pyrc, K., Bosch, B.J., Berkhout, B., Jebbink, M.F., Dijkman, R., Rottier, P., Van Der Hoek, L., 2006. Inhibition of human coronavirus NL63 infection at early stages of the replication cycle. Antimicrob. Agents Chemother. 50, 2000–2008.

Rachidi, N., Taly, J.F., Durieu, E., Leclercq, O., Aulner, N., Prina, E., Pescher, P., Notredame, C., Meijer, L., Spath, G.F., 2014. Pharmacological assessment defines *Leishmania* donovani casein kinase 1 as a drug target and reveals important functions in parasite viability and intracellular infection. Antimicrob. Agents Chemother. 58, 1501–1515.

Reinders, M.K., Van Roon, E.N., Jansen, T.L., Delsing, J., Griep, E.N., Hoekstra, M., Van De Laar, M.A., Brouwers, J.R., 2009. Efficacy and tolerability of urate-lowering drugs in gout: a randomised controlled trial of benzbromarone versus probenecid after failure of allopurinol. Ann. Rheum. Dis. 68, 51–56.

Resta, S., Luby, J.P., Rosenfeld, C.R., Siegel, J.D., 1985. Isolation and propagation of a human enteric coronavirus. Science 229, 978–981.

Romero, M.R., Serrano, M.A., Efferth, T., Alvarez, M., Marin, J.J., 2007. Effect of cantharidin, cephalotaxine and homoharringtonine on "in vitro" models of hepatitis B virus (HBV) and bovine viral diarrhoea virus (BVDV) replication. Planta Med. 73, 552–558.

Rossignol, J.F., La, F.S., Chiappa, L., Ciucci, A., Santoro, M.G., 2009. Thiazolides, a new class of anti-influenza molecules targeting viral hemagglutinin at the post-translational level. J. Biol. Chem. 284, 29798–29808.

Rota, P.A., Oberste, M.S., Monroe, S.S., Nix, W.A., Campagnoli, R., Icenogle, J.P., Penaranda, S., Bankamp, B., Maher, K., Chen, M.H., Tong, S., Tamin, A., Lowe, L., Frace, M., Derisi, J.L., Chen, Q., Wang, D., Erdman, D.D., Peret, T.C., Burns, C., Ksiazek, T.G., Rollin, P.E., Sanchez, A., Liffick, S., Holloway, B., Limor, J., Mccaustland, K., Olsen-Rasmussen, M., Fouchier, R., Gunther, S., Osterhaus, A.D., Drosten, C., Pallansch, M.A., Anderson, L.J., Bellini, W.J., 2003. Characterization of a novel coronavirus associated with severe acute respiratory syndrome. Science 300, 1394–1399.

Saijo, M., Morikawa, S., Fukushi, S., Mizutani, T., Hasegawa, H., Nagata, N., Iwata, N., Kurane, I., 2005. Inhibitory effect of mizoribine and ribavirin on the replication of severe acute respiratory syndrome (SARS)-associated coronavirus. Antiviral Res. 66, 159–163.

Sattar, S.A., Raphael, R.A., Lochnan, H., Springthorpe, V.S., 1983. Rotavirus inactivation by chemical disinfectants and antiseptics used in hospitals. Can. J. Microbiol. 29, 1464–1469.

Seguin, S.P., Ireland, A.W., Gupta, T., Wright, C.M., Miyata, Y., Wipf, P., Pipas, J.M., Gestwicki, J.E., Brodsky, J.L., 2012. A screen for modulators of large T antigen's ATPase activity uncovers novel inhibitors of simian virus 40 and BK virus replication. Antiviral Res. 96, 70–81.

Shi, Z., Wei, J., Deng, X., Li, S., Qiu, Y., Shao, D., Li, B., Zhang, K., Xue, F., Wang, X., Ma, Z., 2014. Nitazoxanide inhibits the replication of Japanese encephalitis virus in cultured cells and in a mouse model. Virol. J. 11, 10.

Siddiq, D.M., Koo, H.L., Adachi, J.A., Viola, G.M., 2011. Norovirus gastroenteritis successfully treated with nitazoxanide. J. Infect. 63, 394–397.

Sinclair, D.S., Fox, I.H., 1975. The pharmacology of hypouricemic effect of benzbromarone. J. Rheumatol. 2, 437–445.

Sorensen, M.D., Sorensen, B., Gonzalez-Dosal, R., Melchjorsen, C.J., Weibel, J., Wang, J., Jun, C.W., Huanming, Y., Kristensen, P., 2006. Severe acute respiratory syndrome (SARS): development of diagnostics and antivirals. Ann. N. Y. Acad. Sci. 1067, 500–505.

Stevenson, G.W., Hoang, H., Schwartz, K.J., Burrough, E.R., Sun, D., Madson, D., Cooper, V.L., Pillatzki, A., Gauger, P., Schmitt, B.J., Koster, L.G., Killian, M.L., Yoon, K.J., 2013. Emergence of porcine epidemic diarrhea virus in the United States: clinical signs, lesions, and viral genomic sequences. J. Vet. Diagn. Invest. 25, 649–654.

Tebas, P., Powderly, W.G., 2000. Nelfinavir mesylate. Expert Opin. Pharmacother. 1, 1429–1440.

Walson, J.L., Otieno, P.A., Mbuchi, M., Richardson, B.A., Lohman-Payne, B., Macharia, S.W., Overbaugh, J., Berkley, J., Sanders, E.J., Chung, M.H., John-Stewart, G.C., 2008. Albendazole treatment of HIV-1 and helminth co-infection: a randomized, double-blind, placebo-controlled trial. AIDS 22, 1601–1609.

Wang, L., Byrum, B., Zhang, Y., 2014. New variant of porcine epidemic diarrhea virus, United States, 2014. Emerg. Infect. Dis. 20, 917–919.

White Jr., A.C., 2003. Nitazoxanide: an important advance in anti-parasitic therapy. Am. J. Trop. Med. Hyg. 68, 382–383.

WHO, 2014. WHO MERS-CoV. <http://www.who. int/csr/don/2014_05_23_mers/en>.

Zhang, X.D., 2007. A pair of new statistical parameters for quality control in RNA interference high-throughput screening assays. Genomics 89, 552–561.

Zhang, X.M., Herbst, W., Kousoulas, K.G., Storz, J., 1994. Biological and genetic characterization of a hemagglutinating coronavirus isolated from a diarrhoeic child. J. Med. Virol. 44, 152–161.

Zhang, X.M., Kousoulas, K.G., Storz, J., 1991. Comparison of the nucleotide and deduced amino acid sequences of the S genes specified by virulent and avirulent strains of bovine coronaviruses. Virology 183, 397–404.

Zhu, H., Yu, D., Zhang, X., 2009. The spike protein of murine coronavirus regulates viral genome transport from the cell surface to the endoplasmic reticulum during infection. J. Virol. 83, 10653–10663.

Please cite this article in press as: Cao, J., et al. A screen of the NIH Clinical Collection small molecule library identifies potential anti-coronavirus drugs. Antiviral Res. (2014), http://dx.doi.org/10.1016/j.antiviral.2014.11.010